^{13}C NMR study of orientational ordering in the chiral-*C* phase of partially deuterated smectic liquid crystals

Ronald Y. Dong,[1,2] J. Xu,[2] J. Zhang,[2] and C. A. Veracini[3]
[1]*Department of Physics and Astronomy, Brandon University, Brandon, MB, Canada R7A 6A9*
[2]*Department of Physics and Astronomy, University of Manitoba, Winnipeg, MB, Canada R3 T 2N2*
[3]*Dipartimento di chimica e chimica Industriale, Universita degli Studi Pisa, Via Risorgimento 35, 56126, Pisa, Italy*
(Received 22 February 2005; published 9 December 2005)

Carbon-13 NMR spectroscopy is used to probe the orientational ordering in the tilted chiral smectic phase of two partially deuterated liquid crystals. Quantitative analyses of the chemical shifts of the aromatic carbons in the smectic-*A* and -C^* phases enable us to obtain the location of the long molecular axis of the core and the off-diagonal order parameter S_{01} of the molecular core in the smectic-C^* phase. The advantage of knowing the ordering information of these molecules in their mesophases from deuteron studies is demonstrated in this work, as they can be used to guide the ^{13}C assignments. The temperature behaviors of the ^{13}C chemical shifts from the aromatic sites in the helical structure of the smectic-C^* phase is caused by both an increase of the tilt angle and a change in the orientation of the principal frame that describes the molecular ordering.

DOI: 10.1103/PhysRevE.72.061701 PACS number(s): 61.30.−v

I. INTRODUCTION

Chirality has played an important role in liquid crystal (LC) research. Molecular chirality can come from asymmetric carbon site(s) in LC molecules, and together with their lateral electric dipoles can give rise to unique phase structures. These materials can show ferroelectric, antiferroelectric, and/or ferrielectric, as well as unique optical properties [1–3]. Bent-core molecules do not contain chiral carbon sites, but may also form chiral LC phases. Because of their noncylindrical molecular cores and effective packing within layers of tilted smectic phases, in-layer electric polarization, and ferroelectric properties have been observed in bent-core mesogens [4]. Recently, we have combined deuteron and ^{13}C NMR to study the nematic phase of a bent-core mesogen [5], and found that the correct assignment of ^{13}C lines and precise chemical shift tensors for carbon sites are essential for extracting order parameters and structural information. One- and two-dimensional ^{13}C NMR techniques have been shown in studies of other bent-core molecules [6,7] in their nematic phases.

Chiral LCs have been studied in the past by means of ^{13}C [8–10] and ^{2}H [11–15] NMR spectroscopy. It has been found in these studies that some aromatic carbon lines suffer marked line broadening when entering the ferroelectric phase, and similar broadening of ^{2}H quadrupolar doublets from the deuterons located near the top of a chain has also been observed. One reason of line broadening could be due to possible distortions of the helicoidal structure by the external magnetic field. It would be of interest to determine the exact cause(s) of line broadenings, e.g., dynamics of molecules, or distortion of their distributions within the layered structure. The present study aims to further the understanding of this type of mesogens. ^{13}C NMR study of partially deuterated chiral smectogens can be advantageous, since the spectral assignment of ^{13}C NMR peaks may be guided by the structural and ordering information already available from ^{2}H NMR spectroscopy. To this end, we have carried out ^{13}C NMR in the Sm-*A* and Sm-C^* phase of two smectogens (*S*) [4-(2-methylbutyl)phenyl]-4′-*n*-octylbiphenyl carboxylate (8BEF5), deuterated in the phenyl ring and the attached chiral chain, and 1-methylheptyl 4′-(4-*n*-decyloxybenzoyloxy) biphenyl-4-carboxylate (10B1M7), deuterated at the achiral decyloxy chain. The orientational ordering is examined in the Sm-*A* and ferroelectric Sm-C^* phase of these semctogens. The paper is organized as follows. Section II describes a general theory of chemical shift anisotropies in aligned LC samples, which accounts for both molecular and phase biaxial order parameters. It is noted that in general there are 25 orientational order parameters to describe a tilted smectic phase. In practice, a total of nine order parameters may suffice under certain simplifying assumptions [16,17]. Section III outlines the experimental method, while Sec. IV gives results and discussion. The last section contains a brief summary.

II. THEORY

Here we extend the treatment of time-averaged quadrupolar Hamiltonian in biaxial mesophases given by Doane [16] to give a time-averaged chemical shift Hamiltonian. In the high-field limit,

$$\bar{H}_{\mathrm{CS}} = \gamma\hbar B I_z \delta_{\mathrm{iso}} + \sqrt{\frac{2}{3}}\gamma\hbar B I_z \langle R_{20}\rangle, \tag{1}$$

where the bar over the Hamiltonian denotes the time average due to internal bond rotations and overall motions of the molecule $\langle R_{2m}\rangle$ is the corresponding time-averaged second rank irreducible spherical tensor which describes the spatial parts of the spin Hamiltonian, and $\delta_{\mathrm{iso}}=(\delta_{11}+\delta_{22}+\delta_{33})/3$, with δ_{ii} being the principal components of the chemical shift tensor. Suppose the director $\hat{n}$ (which defined z_N axis of the director frame) is oriented with respect to the *B* field (the laboratory frame) through the Euler angles $(\phi_0, \theta_0, \psi_0)$. In

the present study, we focus on carbon sites located in the molecular core (i.e., phenyl and/or biphenyl fragments). To allow for internal motions of the fragment and overall motions of the molecule, the chemical shift tensor in the principal axis system (PAS) frame must be transformed through successive coordinate transformations to the laboratory frame, i.e., director frame to a molecular frame via (ϕ,θ,ψ), molecular frame to a local (fragment) frame via a set of time-independent (assumed) Euler angles $(\alpha_F,\beta_F,\gamma_F)$, and finally from the fragment frame to the PAS frame via $(0,\beta,90°)$. Hence, one obtains

$$\langle R_{20}\rangle = \sum_{m1}\sum_{m2}\sum_{m3}\sum_{m} D_{m1,0}(\phi_0,\theta_0,\psi_0)\langle D^*_{m1,m2}(\phi,\theta,\psi)\rangle \times D^*_{m2,m3}(\alpha_F,\beta_F,\gamma_F)D^*_{m3,m}(0,\beta,\pi/2)\rho_{2,m}, \quad (2)$$

where in the PAS(1, 2, 3) frame

$$\rho_{20} = \sqrt{\frac{3}{2}}(\delta_{33}-\delta_{\rm iso}), \quad \rho_{2,\pm1}=0, \quad \rho_{2,\pm2}=\frac{1}{2}(\delta_{11}-\delta_{22})$$

The fragment and molecular frames are chosen such that α_F=90° [see Fig. 1(c)] and a set of order parameters is obtained in accordance with Doane's definitions [16]. Also we set γ_F=0 for simplicity in the derivation. The observed chemical shift for a particular carbon site in a mesophase can be expressed (see the Appendix) in terms of three temperature-dependent coefficients a, b, and c:

$$\langle\delta\rangle = \delta_{\rm iso} + a\left(\sqrt{\frac{2}{3}}P_2(\cos\beta_F)R'_{2,0} + (\sin^2\beta_F)R'_{2,2}\right) + b\left(\sqrt{\frac{3}{8}}(\sin 2\beta_F)R'_{2,0} - \frac{1}{2}(\sin 2\beta_F)R'_{2,2}\right) + c\left(\sqrt{\frac{3}{8}}(\sin^2\beta_F)R'_{2,0} + \frac{1}{2}(1+\cos^2\beta_F)R'_{2,2}\right), \quad (3)$$

where a, b, c are expressed in terms of orientational order parameters S_{mn} as

$$a = P_2(\cos\theta_0)S_{00} + \frac{3}{4}\sin(2\theta_0)\sin(\phi_0)S_{10} + \frac{3}{4}\sin^2\theta_0\cos(2\phi_0)S_{20},$$

$$b = P_2(\cos\theta_0)S_{01} + \sin(2\theta_0)\sin(\phi_0)S_{11} - \sin^2\theta_0\cos(2\phi_0)S_{21},$$

$$c = -P_2(\cos\theta_0)S_{02} + \sin(2\theta_0)\sin(\phi_0)S_{12} - \sin^2\theta_0\cos(2\phi_0)S_{22}, \quad (4)$$

and

$$R'_{2,0} = \sqrt{\frac{2}{3}}\left[P_2(\cos\beta)(\delta_{zz}-\delta_{yy}) + \frac{1}{2}(\delta_{yy}-\delta_{xx})\right],$$

$$R'_{2,\pm2} = \frac{1}{2}\{(\sin^2\beta)\delta_{zz} + (\cos^2\beta)\delta_{yy} - \delta_{xx}\}. \quad (5)$$

It is noted that fast 180° flips of the ring render

$$R'_{2,\pm1} = 0.$$

Now the nine orientational order parameters S_{mn} used to describe ordering of a molecular frame in a biaxial mesophase are defined [16] as follows:

$$S_{00} = \langle P_2(\cos\theta)\rangle = S_{zz},$$

$$S_{01} = \langle\sin(2\theta)\sin\psi\rangle,$$

$$S_{02} = \langle\sin^2\theta\cos(2\psi)\rangle = \frac{2}{3}(S_{xx}-S_{yy}),$$

$$S_{20} = \langle\sin^2\theta\cos(2\phi)\rangle,$$

$$S_{21} = \left\langle \sin\theta\sin 2\phi\cos\psi + \frac{1}{2}\sin 2\theta\cos 2\phi\sin\psi\right\rangle,$$

$$S_{22} = \left\langle \frac{1}{2}(1+\cos^2\theta)\cos 2\phi\cos 2\psi - \cos\theta\sin 2\phi\sin 2\psi\right\rangle,$$

$$S_{10} = \langle\sin 2\theta\sin\phi\rangle,$$

$$S_{11} = \langle\cos\theta\cos\phi\cos\psi - \cos 2\theta\sin\phi\sin\psi\rangle,$$

$$S_{12} = \left\langle \sin\theta\cos\phi\sin 2\psi + \frac{1}{2}\sin 2\theta\sin\phi\cos 2\psi\right\rangle. \quad (6)$$

In the above equation, the first three expressions except S_{00} reflect the molecular biaxiality, while the remaining expressions reflect the phase biaxiality. If the molecule has a fragment which contains the most ordered axis such that this axis is along the long molecular z_M axis (β_F=0), Eq. (3) reduces to

$$\langle\delta\rangle = \delta_{\rm iso} + \sqrt{\frac{2}{3}}aR'_{2,0} + cR'_{2,2}. \quad (7)$$

Hence the observed chemical shifts of this fragment should in principle contain information on biaxial order parameters S_{10}, S_{20}, S_{12}, and S_{22} in tilted smectic phases. Of course, some of them may not be large to be significant. For the chiral smectogens studied here, the layers in the Sm-C^* phase are normal to the magnetic field and θ_0 is the tilt angle of the molecule with respect to the planar normal. In the past, deuterium and ^{14}N NMR have been exploited to study these biaxial order parameters in the Sm-C and other tilted phases [18,19]. When the phase biaxiality is too small to be important, Eq. (3) reduces to

$$\langle\delta\rangle = \delta_{\rm iso} + P_2(\cos\theta_0)\left\{\left(\sqrt{\frac{2}{3}}P_2(\cos\beta_F)R'_{2,0} + (\sin^2\beta_F)R'_{2,2}\right)S_{00} + \left(\sqrt{\frac{3}{8}}(\sin 2\beta_F)R'_{2,0} - \frac{1}{2}(\sin 2\beta_F)R'_{2,2}\right)S_{01} - \left(\sqrt{\frac{3}{8}}(\sin^2\beta_F)R'_{2,0}\right.\right.$$

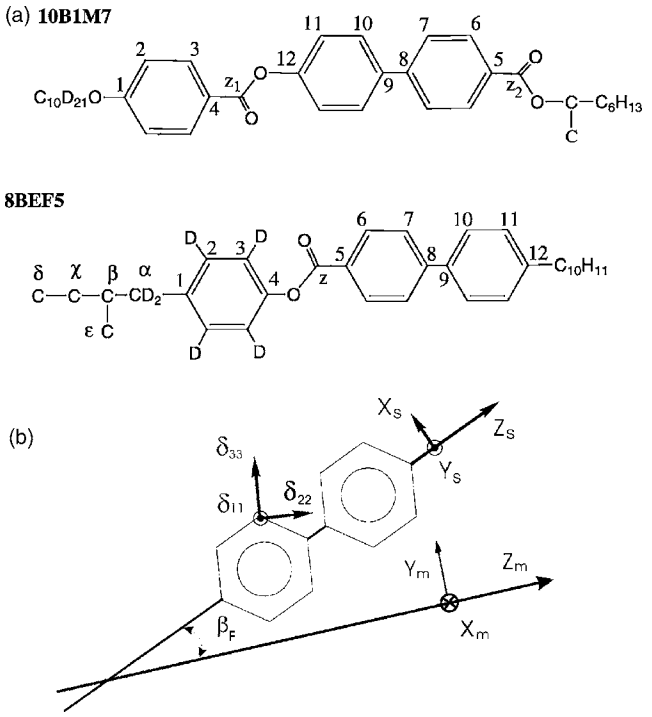

FIG. 1. (a) Molecular formula of partially deuterated 10B1M7 and 8BEF5 (not fully deuterated sites of the chiral chain are not shown explicitly) with carbon site labels. (b) A schematic of the principal axis system of a carbon chemical shift tensor $(\delta_{11}, \delta_{22}, \delta_{33})$, a fragment coordinate system (x_s, y_s, z_s), and the molecular coordinate system (x_M, y_M, z_M).

$$+\frac{1}{2}(1+\cos^2\beta_F)R'_{2,2}\Big)S_{02}\Big\}. \tag{8}$$

This equation appears to be suitable for the Sm-C^* phase of our studied samples. In the Sm-A phase, the director is aligned along the magnetic field (θ_0=0). S_{01} vanishes if the chosen molecular frame is the principal frame of the order matrix, and one obtains

$$\langle\delta\rangle = \delta_{\rm iso} + \left(\sqrt{\frac{2}{3}}P_2(\cos\beta_F)R'_{2,0} + (\sin^2\beta_F)R'_{2,2}\right)S_{00} - \left(\sqrt{\frac{3}{8}}(\sin^2\beta_F)R'_{2,0} + \frac{1}{2}(1+\cos^2\beta_F)R'_{2,2}\right)S_{02}, \tag{9}$$

where $R'_{2,0}$ and $R'_{2,2}$ are again given by Eq. (5). Figure 1 shows the molecular structure of 10B1M7 and 8BEF5 together with their carbon site labels, as well as various coordinate systems used in the above derivation based on coordinate transformations.

III. EXPERIMENTAL

The partially deuterated samples 8BEF5 and 10B1M7, were those used in our previous deuteron NMR studies [12,15]. The NMR experiments were performed on a Bruker Avance 400 spectrometer operating at 100.6 MHz for ^{13}C and 61.4 MHz for ^{2}H. The 1D isotropic ^{13}C spectrum was obtained with a two-channel HX solid probe using a single carbon 90° pulse, and the free induction decay (FID) was collected with Waltz-16 proton decoupling sequence. The ^{13}C spectra in the nematic phase were collected using standard cross polarization (CP) for 2 ms after a 90° proton irradiation. The ^{1}H 90° pulse width was 3.1 μs. Proton decoupling during the ^{13}C signal acquisition was accomplished with the SPINAL-64 pulse sequence [20] having a decoupling field of 40.4 kHz. To avoid sample heating, the recycle delay between each FID acquisition was 7 s. Each spectrum was obtained by signal averaging 128 or 256 scans. The temperature calibration of carbon data was carried out at a given air flow using the known temperature-dependent quadrupolar splittings of the studied liquid crystal. The ^{13}C peak assignments in the aligned sample were based on experiments using a pulse sequence containing phase inversion (PI) and CP (i.e., CPPI) [21], as well as based on ^{13}C peak assignments previously found in similar compounds [9,10]. In the CPPI spectrum, negative CH_2, null CH and positive nonprotonated C signals were used for the spectral discrimination. In addition, two-dimensional (2D) separated local field (SLF) NMR spectrum (Fig. 2) was used to ascertain the assignment of ^{13}C peaks in 10B1M7. The dipolar oscillations were observed on the CP buildup curves, while homonuclear decoupling of protons was achieved by the frequency-switched Lee-Goldburg (FSLG-2) sequence [22,23] at a decoupling strength of 50.9 Hz. The LG decoupling during CP produced a theoretical scaling factor (0.82) for the dipolar oscillation frequency. During the t_2 period, heteronuclear decoupling was achieved by SPINAL-64 at a decoupling field of 40.4 kHz. To decrease the central peaks in the 2D SLF spectrum, a normal cross polarization inversion [24,25] of a fixed duration (2 ms) was included in the pulse sequence.

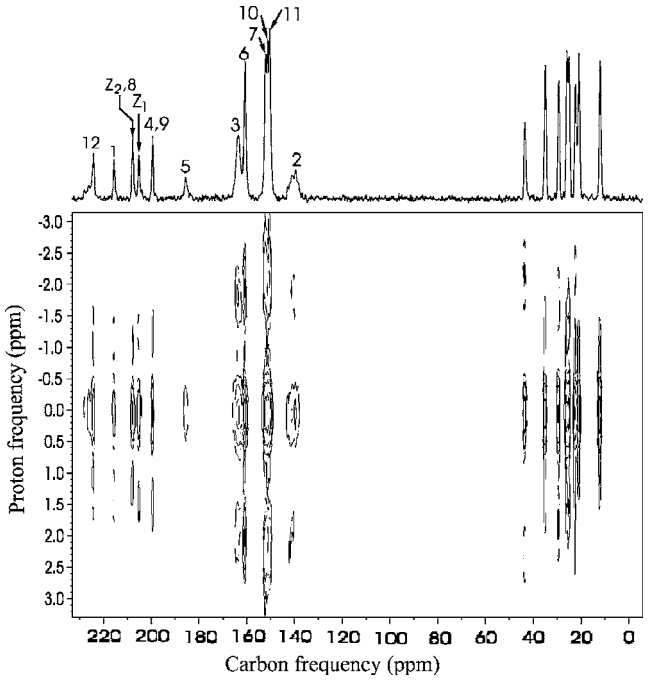

FIG. 2. A typical SLF spectrum recorded in the SmA phase of 10B1M7 at 378 K.

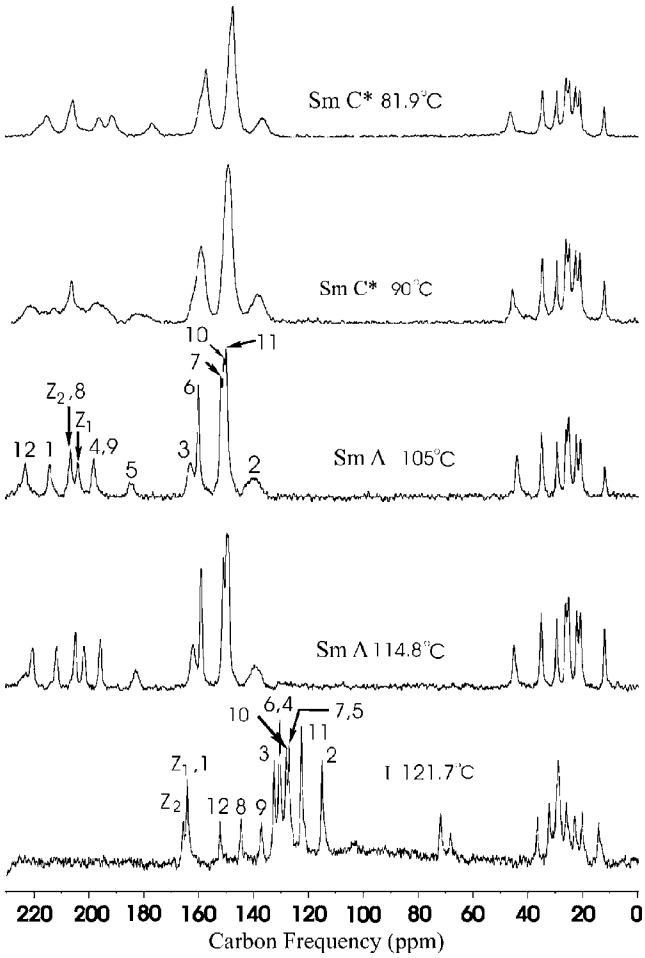

FIG. 3. Typical ^{13}C spectra observed in the aligned sample of 10B1M7 at several temperatures by cooling from the isotropic phase. The carbon peak assignments in isotropic and smectic phases are indicated.

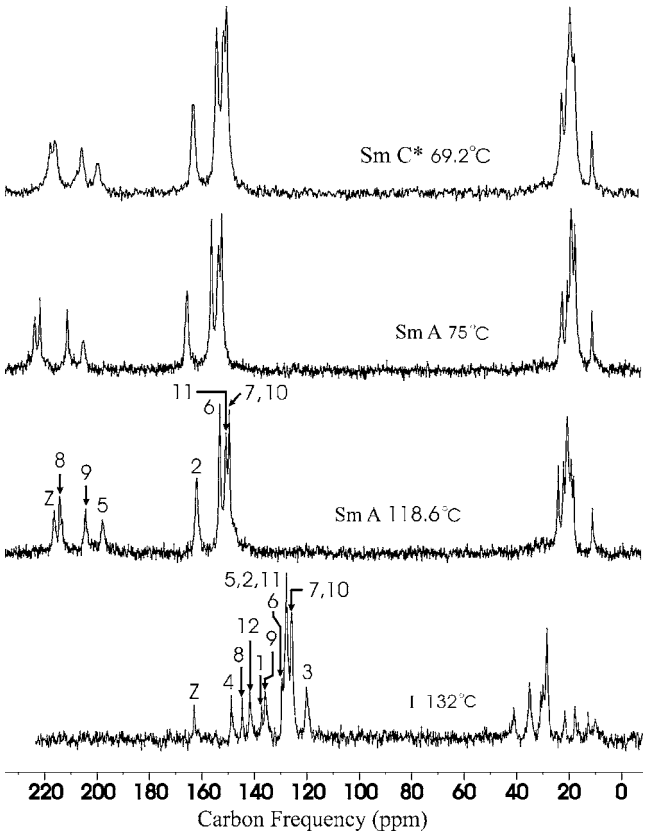

FIG. 4. Typical ^{13}C spectra observed in the aligned sample of 8BEF5 at several temperatures by cooling from the isotropic phase. The carbon peak assignments in isotropic and smectic phases are indicated.

The number of t_1 increments was 32 with 32 scans per t_1 increment, and the STATES method was used. Typical proton and carbon 90° pulse widths in SLF experiments were 3.1 and 4.9 μs, respectively. The temperature gradient across the sample was estimated to be within 0.3°.

IV. RESULTS AND DISCUSSION

We have carried out 1D and 2D ^{13}C NMR measurements in an aligned sample of partially deuterated 10B1M7, and 1D ^{13}C experiments on partially deuterated 8BEF5. The achiral chain of 10B1M7 was deuterated, but this did not influence the observation of aromatic carbon peaks. In 8BEF5, the phenyl carbons could not be as easily detected through cross polarization due to the ring deuteration. Since changes in chain carbon chemical shifts are considerably less upon entering the ordered phases, the present study focuses on the chemical shifts observed from the aromatic parts of these two chiral smectogens. Figures 3 and 4 show some typical ^{13}C spectra with peak assignments recorded at several different temperatures in 10B1M7 and 8BEF5, respectively. It is seen that the ^{13}C lines are broadened in the Sm-C^* phase. Let us first look at the local order parameter matrices [i.e., set β_F=0 in Eq. (9)] of the phenyl and biphenyl fragments derived from the carbon chemical shift data, and compare with the corresponding values obtained from the deuteron data. Here the "molecular" frame is identical to the local fragment frame attached to the studied fragment. Figure 5 shows the local order parameter S'_{zz} for the two molecules versus temperature based on Eq. (9), and chemical shift tensors listed in Table I for 10B1M7 and Table II for 8BEF5. The choice of shift tensors is based on those found in similar LC and model compounds in the literature. For 8BEF5, the phenyl S'_{zz} cannot be obtained from the carbon peaks due to the ring deuteration, and its value is reproduced from the deuteron data [15]. As seen in this figure, the transition from Sm-A to Sm-C^* phase is clearly delineated for both samples. Furthermore, the S'_{zz} value of the phenyl ring is higher than that of the biphenyl fragment for the two molecules. In 10B1M7, S'_{zz} values of the phenyl and biphenyl fragments compare well with those derived from the deuteron splitting data [11], thereby supporting our ^{13}C peak assignments in the aromatic region. The derived local S'_{02} values are not shown here. It is important to point out that Eq. (9) is strictly correct only for the Sm-A phase, since the gradual decreasing S'_{zz} for the phenyl and biphenyl fragments in the tilted Sm-C^* phase, however, show dissimilar temperature behaviors. Thus, the observed S'_{zz} behaviors in the Sm-C^* phase with decreasing temperature may well be due to the temperature-dependent

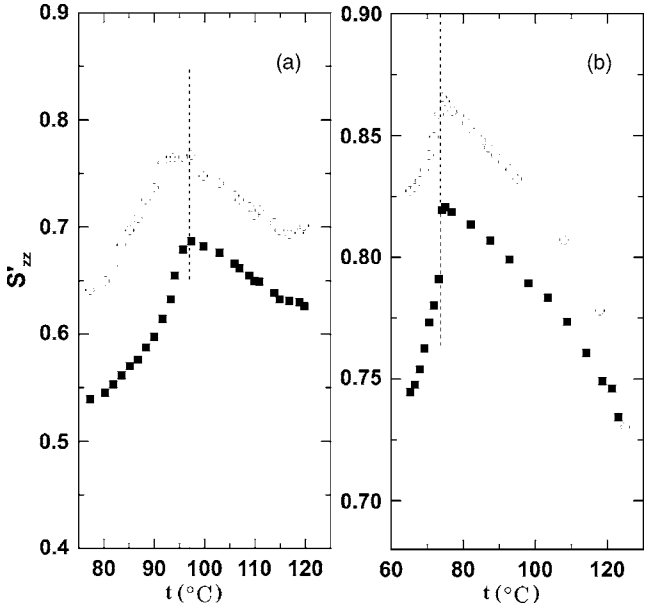

FIG. 5. Plot of local nematic order parameter S_{zz} in the Sm-A and Sm-C^* phase of (a) 10B1M7 and (b) 8BEF5. Open and closed symbols denote phenyl and biphenyl fragments, respectively.

tilt angle. A proper treatment of molecular order parameters in the Sm-C^* phase is required and will be considered below.

From the two local S'_{zz} values of the phenyl and biphenyl fragments at each temperature, one can calculate the angle between their para axes in the Sm-A phase. An average angle of 14.4° was estimated for 10B1M7. This is slightly smaller than that given before [11]. A value of 15° is assumed for the angle between the para axes in 8BEF5, since the molecular cores of 10B1M7 and 8BEF5 are quite similar, but not identical. Based on this information, one can then determine the location of the long z_M axis for the molecular core in term of β_F^{biph} and β_F^{ph}. Since $P_2(\cos\beta_F^{\text{ph}})/P_2(\cos\beta_F^{\text{biph}}) = S'_{zz}(\text{ph})/S'_{zz}(\text{biph})$, the average β_F^{ph} is found to be around 0.1° in 10B1M7, indicating that the phenyl para axis is nearly the most ordered axis of the molecular core, a conclusion made in a previous deuteron study [11]. The average β_F^{ph} in 8BEF5 is found as around 5.2°. In the following calculations, we assume a constant average β_F^{ph} for these mesogens over the range of studied temperature. Since the core z_M axis is known, it is more useful to discuss the orientational ordering of the molecular core in terms of S_{00}, S_{02}, and S_{01}, using a molecular (M) axis system (x_M, y_M, z_M). Even though z_M is known, the choice of y_M in the x_S, z_S plane on the biphenyl fragment can only be justified by additional experimental evidence (see below). In Sm-A phase, the temperature behaviors of the S'_{zz}'s of the phenyl and biphenyl fragments are found to be identical without S_{01}, while in the Sm-C^* phase, a nonzero S_{01} is probably responsible for the observed different temperature behaviors of S'_{zz}'s.

TABLE I. Chemical shift tensors in ppm of 10B1M7 (values in parentheses are experimental and within an accuracy of about 3 ppm).

Carbon	δ_{11}	δ_{22}	δ_{33}	δ_{iso}	Ref.
C2	18.7	131.7	184.7	111.7 (114.9)	[26]
C3	15	153	226	131.3 (132.4)	[26]
C4	14.6	147.4	219.3	127.1 (130.4)	[27]
C5	14.6	147.4	219.3	127.1 (126.9)	[27]
C6	15	153	226	131.3 (130.4)	[28]
C7	21.3	150.2	200.8	124.1 (126.9)	[10]
C8	20	173	236	143 (144.6)	[10]
C9[a]	14.4	169.1	235.9	139.8 (137.1)	[27]
C10	21.8	145.5	217.9	128.4 (128.1)	[10]
C11	30	149.3	183.0	120.8 (122.5)	[7]
C12	71.7	137.4	225.9	155 (152.1)	[10]

[a]Theoretical shielding tensor from Ref. [27].

TABLE II. Chemical shift tensors in ppm of 8BEF5 (values in parentheses are experimental and within an accuracy of about 3 ppm).

Carbon	δ_{11}	δ_{22}	δ_{33}	δ_{iso}	Ref.
C5	8.7	155.7	227.7	130.7 (128.8)	[26]
C6	28.3	145.7	212.7	128.9 (129.8)	[7]
C7	21.3	150.2	200.8	124.1 (126.2)	[10]
C8	20	173	236	143 (145)	[10]
C9[a]	14.4	169.1	235.9	139.8 (136.4)	[27]
C10	21.8	145.5	217.9	128.4 (126.2)	[10]
C11	9.7	138.7	237.7	128.7 (128.1)	[26]

[a]Theoretical shielding tensor from Ref. [27].

A. 10B1M7

A typical 2D SLF spectrum, shown in Fig. 2, gives a proton-decoupled ^{13}C peaks in the f_2 dimension, while the slices in the f_1 dimension show the individual ^{13}C nuclei with the C-H dipolar couplings (for which the scaling factor due to FSLG-2 has not been accounted). We have carried this experiment at several temperatures. The spectrum is particularly useful to assign the z peaks, since the C-H dipolar coupling for the z carbons is slightly less than those for the quaternary carbons such as C1, C4, C5, C8, and C9 based on their carbon-proton distances. Figure 6 shows a plot of the aromatic ^{13}C shifts versus temperature in the Sm-A and Sm-C^* phase of 10B1M7. The carbon labels are those indicated in Fig. 1. Using $\beta_F^{\text{biph}}=14.2°$ and $\beta_F^{\text{ph}}=0.1°$ in Eq. (9) to fit C_2-C_{12} chemical shifts (C1 is not used due to unavailable shift tensor) in the Sm-A phase, the core order parameter $S_{00}(S_{zz})$ is identical to that of the phenyl fragment [Fig. 5(a)], while S_{02} (or S_{xx}-S_{yy}) is shown in Fig. 7. Typical error limits (see below) of S_{00} are within 0.02, and of S_{02} are shown in Fig. 7. As seen in Fig. 1(c), the molecular frame is chosen with the y_M axis attached on the biphenyl fragment plane (same as in 8BEF5, see below), since the formalism is made particularly simple when the α_F angle is 90°. To allow a possible twist between the biphenyl and phenyl fragments, the corresponding α_F angle for the phenyl carbon sites would be different from the assumed 90°. Strictly speaking Eq. (9)

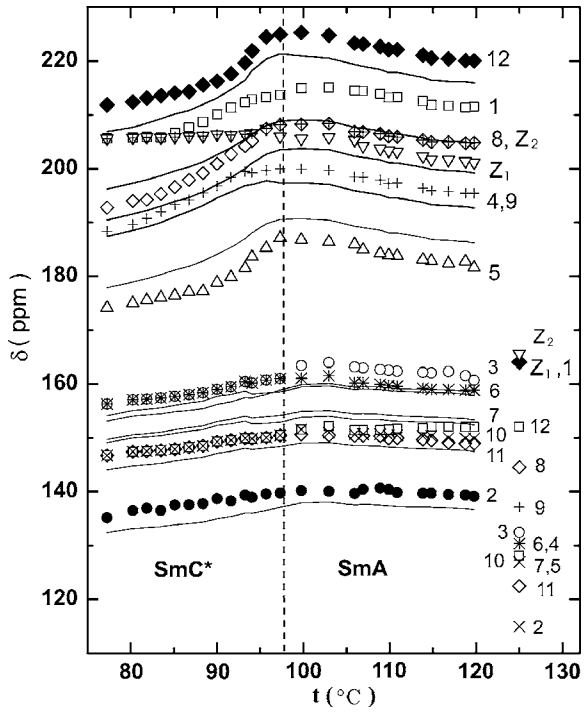

FIG. 6. Plot of chemical shifts of aromatic carbons in the isotropic and smectic phases of 10B1M7. Solid lines denote, starting from the top, theoretical fitting curves for *C*5, *C*9, *C*4, *C*8, *C*12, *C*11, *C*10, *C*7, *C*6, and *C*2, while dashed line denotes *C*3.

cannot be used for sites 2–4, but since β_F^{ph} is almost zero, a slight twist between the two fragments would not make Eq. (9) inappropriate for the phenyl carbons. In the Sm-C^* phase, the same procedure is used except Eq. (8) is used when neglecting the phase biaxiality. The S_{zz} values in Sm-C^* phase were fixed to those extrapolated from the S_{zz} values of the phenyl group in Sm-*A* phase, and the tilt angles were also determined from these extrapolated values (see Fig. 8), which are comparable to the tilt angle found in a previous deuteron study [11]. Given the S_{zz} and the tilt angle, the

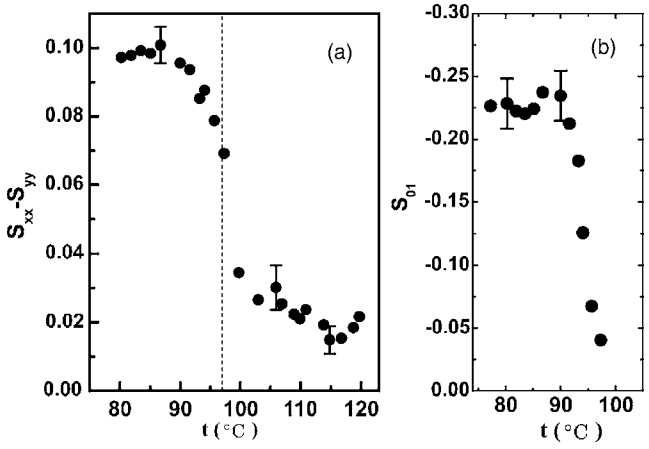

FIG. 7. (a) Plot of the core order parameter S_{xx}-S_{yy} as a function of temperature in smectic-*A* and smectic-C^* phases of 10B1M7, (b) plot of the core order parameter S_{01} in smectic-C^* phase of 10B1M7.

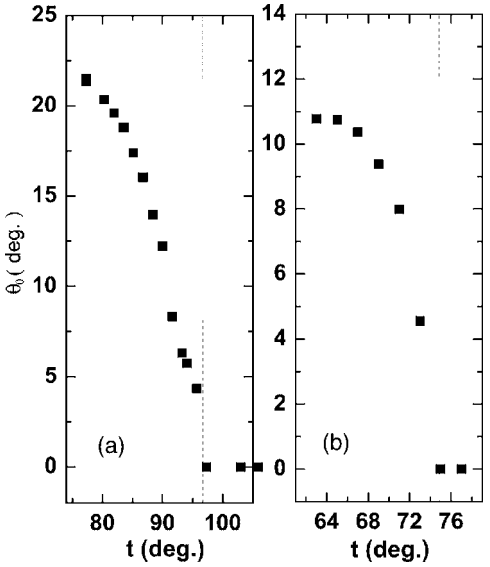

FIG. 8. Plots of tilt angle versus temperature in the Sm-C^* phase of 10B1M7 (a) and 8BEF5 (b).

fitting in the Sm-C^* phase therefore involves only two unknown order parameters S_{xx}-S_{yy} and S_{01}. These derived order parameters are shown in Fig. 7. We note that at the transition into the Sm-C^* phase, S_{01} becomes nonzero and rises to a small plateau value of around −0.2. This indicates that the orientation of PAS of the order matrix has deviated from the chosen *M* frame in the Sm-*A* phase. Furthermore, there appears a discontinuous jump in the molecular biaxial ordering at the Sm-*A*–Sm-C^* transition. The negative S_{01} is simply a result of the choice of x_M and y_M axes. The calculated chemical shifts based on the derived order parameters are shown as solid curves in Fig. 6. The agreement between the experimental and calculated ^{13}C shifts for C_2-C_{12} is acceptable in view of some uncertainties in the chemical shift tensors obtained from the literature.

B. 8BEF5

Figure 9 shows a plot of the aromatic ^{13}C shifts as a function of temperature in the Sm-*A* and Sm-C^* phase of 8BEF5. Using a β_F angle of 9.8° for the biphenyl fragment and Eq. (9) to fit the δ for sites C5 to C11 in the Sm-*A* phase, we have derived the molecular S_{zz} (Fig. 10) and S_{xx}-S_{yy} (Fig. 11) values together with typical error limits. For a direct comparison with the deuteron data [15], the phenyl S'_{zz} is scaled to give the core S_{zz} in Fig. 10. The very good agreement of S_{zz} between the carbon and deuteron data would indicate that the choice of the y_M axis on the biphenyl plane appears to be satisfactory at least for this molecule. The error in order parameters was estimated by fitting the shift data using only sites from one ring in the biphenyl fragment. It is noted that the molecular biaxial order S_{xx}-S_{yy} is relatively insensitive to temperature in this phase. Since our ^{13}C spectra did not seem to show any phase biaxiality in the Sm-C^* phase, we have again used Eq. (8) to determine S_{xx}-S_{yy} and S_{01}, while fixing the S_{zz} values to the extrapolated values from those given in the Sm-*A* phase. The tilt angle is

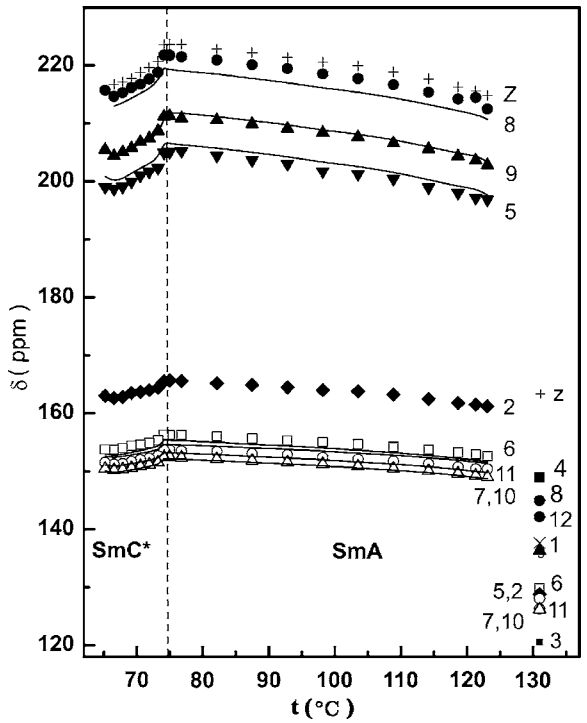

FIG. 9. Plot of chemical shifts of aromatic carbons in the isotropic and smectic phases of 8BEF5. Solid lines denote, starting from the top, theoretical fitting curves for *C*8, *C*9, *C*5, *C*6, *C*11, *C*7, and *C*10.

reproduced from the deuteron work [15] in Fig. 8. The derived S_{xx}-S_{yy} and S_{01}, shown in Fig. 11, are now sensitive to temperature. In comparison with the other mesogen studied here, the S_{01} value is slightly smaller at the same reduced

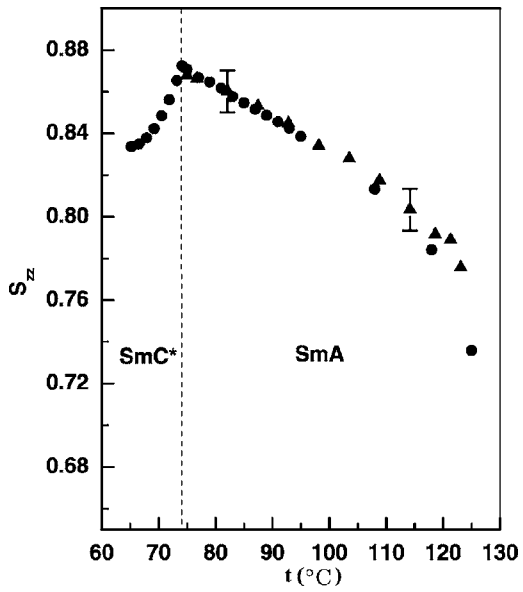

FIG. 10. Plot of the molecular order parameter S_{zz} as a function of temperature for 8BEF5. Solid triangles denote values in the Sm-*A* phase obtained using Eq. (9). Solid circles denote values derived from the deuterium work [15] using the approximate equation $S_{zz}P_2(\cos\beta^{\mathrm{ph}}{}_F)=S'_{zz}$.

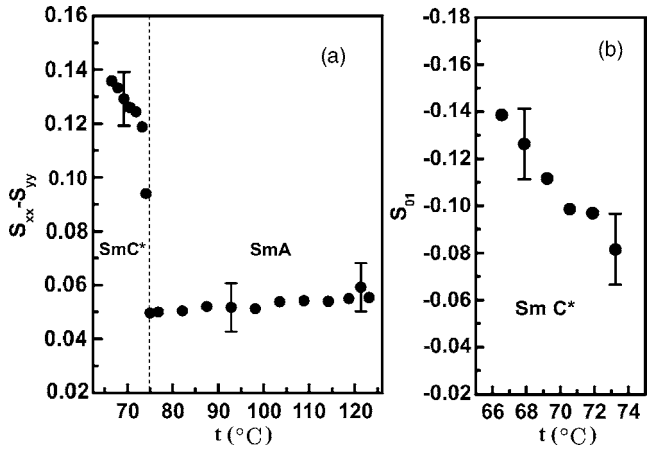

FIG. 11. (a) Plot of the molecular order parameter S_{xx}-S_{yy} as a function of temperature in smectic-*A* and smectic-C^* phases of 8BEF5. (b) Plot of the molecular order parameter S_{01} in smectic-C^* phase of 8BEF5.

temperature. The nonzero S_{01} values again indicate that the chosen *M* frame is not a proper principal frame for the order matrix in the Sm-C^* phase. The calculated ^{13}C shifts based on the derived order parameters are shown as solid curves in Fig. 9 and the fits appear to be reasonable.

V. SUMMARY

The analyses of carbon chemical shift data in the ordered mesophases can, in principle, be useful for obtaining structure and ordering of molecules. Because of possible incorrect peak assignments and difficulty often encountered in picking the proper chemical shift tensors for various carbon sites, the derived molecular information must be taken with care and/or collaborated by complementary information such as those found in the corresponding partially deuterated mesogen when possible. Indeed the present study has demonstrated that reliable ordering information can be obtained by combining carbon and deuteron results. In the Sm-*A* phase of 10B1M7, S_{xx}-S_{yy} increases slightly upon decreasing the temperature, while this is relatively insensitive to temperature in the Sm-*A* phase of 8BEF5. Both samples show a jump in S_{xx}-S_{yy} at the Sm-*A*–Sm-C^* phase transition. Furthermore, in previous deuteron works on these molecules 10B1M7 and 8BEF5, a possible change of the orientation of PAS of the order matrices in the tilted Sm-C^* phase has not been addressed. It would appear that three order parameters are a nature way to describe the orientational ordering of chiral molecules in the tilted smectic phase. Furthermore, S_{xx}-S_{yy} in the Sm-C^* phase for the molecular core of 8BEF5 is slightly larger than that for the molecular core of 10B1M7. We also like to point out that special techniques, such as orienting the pitch axis at a nonzero angle with respect to the magnetic field, are required to detect any phase biaxiality in the Sm-C^* phase. Our preliminary spectral simulation results have indicated that the phase biaxiality in the Sm-C^* phase is indeed negligible in 10B1M7.

ACKNOWLEDGMENTS

We thank the financial support from the Nature Sciences and Engineering Council of Canada, Canada Foundation of Innovation, and Brandon University.

APPENDIX

It is well known that in general five nonzero parameters are needed in an order matrix to describe molecular orientational order in a uniaxial phase (in a principal order tensor frame, the number of order parameter elements reduces to two for a molecule with a nonzero molecular biaxiality), while 25 nonzero order parameters are required to describe molecular ordering in biaxial mesophases. As seen in Sec. II, under certain simplifying assumptions, there are still nine order parameters [Eq. (6)] needed to describe a biaxial phase.

Equation (2) can be rewritten to give

$$\langle R_{20}\rangle = \sum_{m1}\sum_{m2} D_{m1,0}(\phi_0,\theta_0)\langle D^{*}_{m1,m2}(\phi,\theta,\psi)\rangle R''_{2,m2}.$$

Now $m1=0$ gives the following contribution to $\langle R_{20}\rangle$, denoted by I:

$$I = \sqrt{\frac{3}{2}}P_2(\cos\theta_0)\left[\sqrt{\frac{2}{3}}S_{00}R''_{2,0} - S_{01}R''_{2,1} - S_{02}R''_{2,2}\right].$$

This leads to Eq. (8).

To consider phase biaxiality in $\langle R_{20}\rangle$, one must consider contributions due to $m1=1$ and -1, denoted by II, and $m1=2$ and -2, denoted by III. Now, after lengthy arithmetic and using the apolar property of the phase, viz all terms must be invariant when $\theta_0, \phi_0 \rightarrow \pi-\theta_0, \pi+\phi_0(\equiv -\phi_0)$, one obtains

$$III = \sqrt{\frac{3}{2}}\sin^2\theta_0\cos 2\phi_0\left[\sqrt{\frac{3}{8}}S_{20}R''_{2,0} + S_{21}R''_{2,1} - S_{22}R''_{2,2}\right].$$

Similarly, one finds

$$II = \sqrt{\frac{3}{2}}\sin 2\theta_0\sin\phi_0\left[\sqrt{\frac{3}{8}}S_{10}R''_{2,0} - S_{11}R''_{2,1} + S_{12}R''_{2,2}\right],$$

where, for example,

$$R''_{2,0} = P_2(\cos\beta_F)R'_{2,0} + \sqrt{\frac{3}{2}}\sin^2\beta_F R'_{2,\pm 2}.$$

Thus, Eq. (3) in the text can be obtained using

$$\langle \delta_{zz}\rangle = \delta_{\mathrm{iso}} + \sqrt{\frac{2}{3}}\langle R_{20}\rangle.$$

[1] R. B. Meyer, L. Liebert, L. Strezelecki, and P. Keller, J. Phys. (France) Lett. **36**, L69 (1975).

[2] A. P. L. Chandani, Y. Ouchi, H. Takezoe, A. Fukuda, H. Tereshima, K. Furukawa, and A. Kishi, Jpn. J. Appl. Phys., Part 2 **28**, L1261 (1989).

[3] A. Fukuda, Y. Takanishi, T. Isozaki, K. Ishikawa, and H. Takezoe, J. Mater. Chem. **4**, 997 (1994).

[4] T. Niori, F. Sekine, J. Watanabe, T. Furukawa, and H. Takezoe, J. Mater. Chem. **4**, 997 (1996).

[5] R. Y. Dong, K. Fodor-Csorba, J. Xu, V. Domenici, G. Prampolini, and C. A. Veracini, J. Phys. Chem. B **108**, 7694 (2004).

[6] R. Y. Dong, J. Xu, G. Benyei, and K. Fodor-Csorba, Phys. Rev. E **70**, 011708 (2004).

[7] J. Xu, K. Fodor-Csorba, and R. Y. Dong, J. Phys. Chem. A **109**, 1998 (2005).

[8] A. Chen, C.-D. Poon, T. J. Dingermans, and E. T. Samulski, Liq. Cryst. **24**, 255 (1998).

[9] A. Yoshizawa, H. Kikuzaki, and M. Fukumasa, Liq. Cryst. **18**, 351 (1995).

[10] T. Nakai, H. Fujimori, D. Kuwahara, and S. Miyajima, J. Phys. Chem. B **103**, 417 (1999).

[11] D. Catalano, M. Cavazza, L. Chiezzi, M. Geppi, and C. A. Veracini, Liq. Cryst. **27**, 621 (2000).

[12] R. Y. Dong, L. Chiezzi, and C. A. Veracini, Phys. Rev. E **65**, 041716 (2002).

[13] D. Catalano, M. Cifelli, M. Geppi, and C. A. Veracini, J. Phys. Chem. A **105**, 34 (2001).

[14] L. Chiezzi, V. Domenici, M. Geppi, C. A. Veracini, and R. Y. Dong, Chem. Phys. Lett. **358**, 257 (2002).

[15] D. Catalano, L. Chiezzi, V. Domenici, M. Geppi, C. A. Veracini, R. Y. Dong, and K. Fodor-Csorba, Macromol. Chem. Phys. **203**, 1594 (2002).

[16] D. J. Photinos, P. J. Bos, J. W. Doane, and M. E. Neubert, Phys. Rev. A **20**, 2203 (1979).

[17] J. W. Doane, in *Magnetic Resonance of Phase Transitions*, edited by J. Owens, C. P. Poole, Jr., and H. A. Farack (Academic, New York, 1979).

[18] P. J. Bos, A. Shetty, J. W. Doane, and M. E. Neubert, J. Chem. Phys. **73**, 733 (1980).

[19] R. Blinc, J. Seliger, M. Vilfan, and V. Zager, J. Chem. Phys. **70**, 778 (1979).

[20] B. M. Fung, A. K. Khitrin, and K. Ermolaev, J. Magn. Reson. **142**, 97 (2000).

[21] X. Wu and K. W. Zilm, J. Magn. Reson., Ser. A **102**, 205 (1993).

[22] A. Bielecki, A. C. Kolbert, and M. H. Levitt, Chem. Phys. Lett. **155**, 341 (1989).

[23] M. Lee and W. Goldburg, Phys. Rev. **140**, A1261 (1965).

[24] C. H. Wu, J. Magn. Reson., Ser. A **109**, 270 (1994).

[25] N. Sinha and K. V. Ramanathan, Chem. Phys. Lett. **332**, 125 (2000).

[26] D. E. Wemmer, A. Pines, D. D. Whitehurst, Philos. Trans. R. Soc. London, Ser. A **300**, 15 (1981).

[27] G. Zheng, J. Hu, X. Zhang, L. Shen, C. Ye, and G. A. Webb, J. Mol. Struct.: THEOCHEM **428**, 283 (1998).

[28] H. Oulyadi, F. Lauprêtre, and L. Monnerie, Macromolecules **23**, 1965 (1990).